

Military Technical College
Kobry El-Kobbah,
Cairo, Egypt



14th International Conference on
Applied Mechanics and
Mechanical Engineering.

Fatigue-Life Distributions and Failure Probability for Fiber- Reinforced Composite Beams

By

M. Abo- El khier *

A.A.Hamada **

A. Bahei El- Deen***

Abstract:

There has been an upsurge in the application of composite materials in the last few decades, due to high demands on their performance in many applications. Most of these applications include the situations where degradation of strength and life by fatigue process is most likely. In this investigation, plane bending fatigue tests have been conducted on glass/ polyester composite laminates with various lamina orientations to investigate fatigue behavior. It has been observed that the probabilistic distribution of fatigue-life of glass-fiber reinforced composites, at a particular stress level, can be modeled by two-parameter Weibull distribution, with high statistical co-relation coefficient. Two methods have been used to obtain the parameters of Weibull distribution. The two-parameter Weibull distribution has also been employed to incorporate failure probability into S–N relationships. For all considered composite laminates, different modes of failure are observed at low and high fatigue stress levels, which establish different damage mechanisms. The results revealed that higher shape parameters are observed at higher stress levels with less scatter in the fatigue-life data indicating a more uniform damage mechanism.

Keywords:

Fatigue, Composites, Failure Probability, Weibull Distribution

* Professor, Department of production engineering and mechanical design, faculty of engineering, Menoufia University, Shibin El-Kom, Egypt, maboelkhier@hotmail.com

** Associate professor, Department of production engineering and mechanical design, faculty of engineering, Menoufia University, Shibin El-Kom, Egypt, a_ahmed_59@yahoo.com

*** Demonstrator, Department of production engineering and mechanical design, faculty of engineering, Menoufia University, Shibin El-Kom, Egypt, ahmed.bahei@yahoo.com

1. Introduction:

Composite materials are widely used in automotive, naval, and aerospace structures, where they are often subjected to cyclic fatigue loading. Fatigue is one of the most common failure modes in all structural materials, including composite materials. Due to the anisotropic properties of composite materials, the fatigue problem is multiaxial. There is extensive progress in multiaxial fatigue analysis of metals, but much further effort is needed in composite materials [1–4]. Accurate fatigue life prediction needs to include the random variation in material properties (Young's modulus, strength, etc.), loading history, component geometry, and environmental conditions.

Composite materials are inhomogeneous and anisotropic and their behavior in fatigue is more complicated than at of homogeneous and isotropic materials like metals. The main reasons for this are the different types of damage that can occur, i.e., fiber fracture, matrix cracking, fiber buckling and their interactions [5]. Fatigue failure in composites is usually accompanied by extensive damages, which are multiplied through specimen volume instead of a predominant single crack [6].

Glass-fiber reinforced polymer (GFRP) composite materials are used instead of metallic materials because of their low density, high strength, and high rigidity. Therefore, GFRP materials are preferably used in wind turbine blades, in air, sea and land transportation. Most of these materials are subjected to a cycle loading during service conditions. The behavior of composite materials under cycling loading and fracture behavior are really complex [5-8] since, anisotropy structure of GFRP materials forms three dimensional state of stress. Static and fatigue failures in multilayer composites contain different damage mechanisms such as: matrix cracking, fiber–matrix debonding, ply delamination and fiber breakage. The form of each failure type is different depending on material properties, number of layers and loading type [7,9]. Thus, knowing the fatigue behavior under the cyclic loading is essential for using composite materials safely [5–8]. As it is in inhomogeneous all materials, it can be seen great differences in static strength and fatigue life test results among the samples under the same conditions in GFRP composites having anisotropy structure as well. Statistical evaluations are very important because of the different distribution of the test results in GFRP samples [9].

Several mathematical models have been employed to study the statistical dispersion of fatigue-life, for example, Weibull distribution function which has proved to be useful and versatile means for describing composite material properties. The probability density function of the Weibull distribution has a wide variety of shapes [10]. In the present work, the statistical analysis of plane bending fatigue life data in Fiber- Reinforced Composite Beams was investigated by modeling the probabilistic distribution at a particular stress level based on two-parameter Weibull distribution which has also been employed to incorporate failure probability into S–N relationships.

2. Experimental work

2.1 Specimen preparation

Plates of glass fiber reinforced polyester (GFRP) composite with thickness of 3 mm and with different lamina orientations: $[0^\circ]_3$, $[45^\circ]_3$ and $[90^\circ]_3$ were manufactured using the hand lay-up technique and fiber volume fraction was determined experimentally as 0.54%

by firing technique [11]. The constituent of the materials are illustrated in table1. Standard specimens were machined to the dimensions shown in Fig.1.

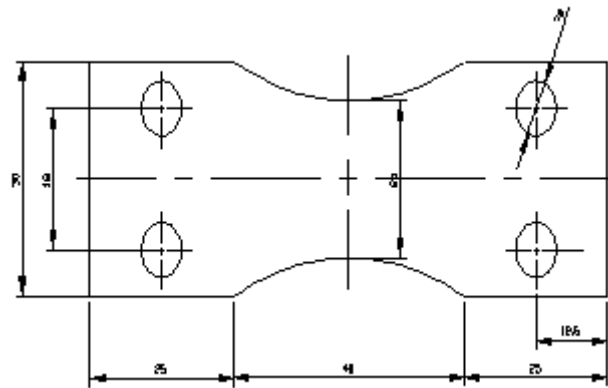


Fig.1. Dimensions of the specimen used for fatigue testing (mm)

Table 1. Specifications of test specimens

Matrix	Orthophthalic polyester resin (QL 8520 A)
Reinforcement	E-roving glass ($\rho_l = 1150 \text{ g/km}$, $d = 17 \pm 2 \text{ }\mu\text{m}$)
Catalyst	Methylethyl ketone peroxide (0.8% of matrix volume)
Hardener	Cobalt naphthenate (0.5% of matrix volume)

2.2. Fatigue tests

The fatigue tests were carried out at the Central Metallurgical R & D Institute (CMRDI), Helwan, Egypt using plane bending fatigue testing machine shown in Fig.2.a. The specifications of the machine are illustrated in table2. The tests were carried out at room temperature. The specimens were subjected to alternate cycles of tensile and compressive stresses as shown in Fig.2.b. Tests were terminated by complete fracture of the specimens. At least three specimens were tested to fracture for each data point on S-N curve. The Ultimate tensile strength (σ_{ult}) values for for GFRP with different lamina orientation along with the Fatigue testing stress levels are listed in Table3.

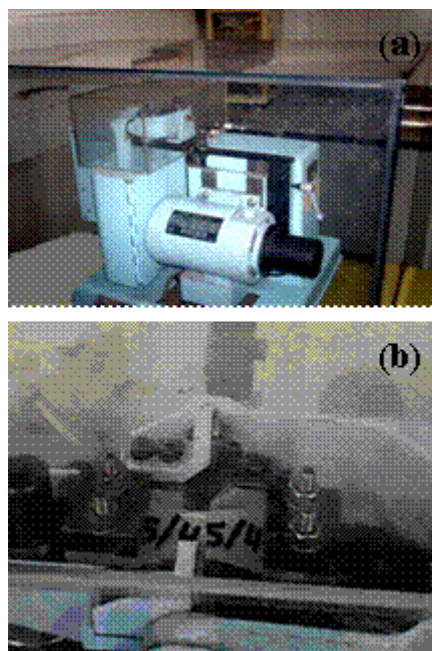


Fig.2 (a) Fatigue test machine, (b) Test specimen during

Table 2. Specifications of the plane bending fatigue testing machine

Bending Moment		30 N.m
Dynamic Moment		±15 N.m
Average Moment		15N.m
Max. Dynamic Angle moment		±15
Max. static Angle Moment		18°
Cycle Speed		300 ~1500 cpm
Displaying Unit	Moment	4 digits
	Speed	4 digits
	No. of cycles per minute	6 digits
Power		0.2 KVA

Table 3. Ultimate tensile strength and fatigue test levels for GFRP with different lamina orientation

Lamina orientation	[0°] ₃	[45°] ₃	[90°] ₃
Ultimate tensile Strength σ_{ult}	35 MPa	25 MPa	20 MPa
Fatigue stress level "σ"	32 MPa(0.91 σ_{ult})	21 MPa(0.84 σ_{ult})	16 MPa(0.80 σ_{ult})
	31 MPa(0.89 σ_{ult})	20 MPa(0.8 σ_{ult})	14 MPa(0.70 σ_{ult})
	30.5 MPa(0.87 σ_{ult})	19.5 MPa(0.76 σ_{ult})	10 MPa(0.5 σ_{ult})
	30 MPa(0.86 σ_{ult})	19 MPa(0.74 σ_{ult})	7 MPa(0.35 σ_{ult})

3. Failure Mechanisms

There are different damage mechanisms occurring in GFRP specimens. Figure 3(a) and (b) shows the photograph of the GFRP specimens after the complete fatigue failure. The mode of failure of GFRP specimens during plane bending fatigue tests is discussed for two cases as follows:

(i) Damage of GFRP specimens of [0°]₃ lamina orientation tested at high stress level of 32 MPa (0.91 σ_{ult}) wherein different damage mechanisms are observed . Longitudinal cracks are produced parallel to the fiber direction at the specimen. Figure 4 shows the scan electron micro-graphs (SEM) image of the failed specimens carried out at the Central Metallurgical R & D Institute (CMRDI), Helwan, Egypt at confidence level of 95%. Figure. 4(a), (b) and(c) shows the SEM image of the failed GFRP specimen of [0°]₃ lamina orientation tested at high stress level. De-bonding and longitudinal matrix cracking is clearly visible as illustrated in Fig.4 (a). This de-bonding along with cracking of the matrix weakens the material and the full load is now carried by fibers only.

Figure 4 (b) shows the SEM image of the cross-section of the failed GFRP specimen. Separation between the fibers due to de-bonding at the fiber matrix interface is clearly visible. The cracks were initiated and propagated at the fiber/matrix interface. The debonded areas around the fibers were connected together through transverse cracks in the matrix, and the final failure was due to shearing of the fibers at plane normal to the specimen axis. Specimens with high stress level have excessive transverse and longitudinal cracks in the matrix. These cracks work as stress concentrator to the fibers at different cross-sections along the fibers resulting in fiber breakage as shown in Fig.4 (c).

(ii) Damage of GFRP specimens of [45°]₃ lamina orientation tested at low stress level of 19 MPa (0.74 σ_{ult}) wherein fiber pull-out and longitudinal cracks are clearly visible as

shown in Fig. 4 d. Longitudinal cracks rapidly travel along the length of the specimen, as shown in Fig.4.b. It is observed that the specimen then fails catastrophically due to fiber pullout

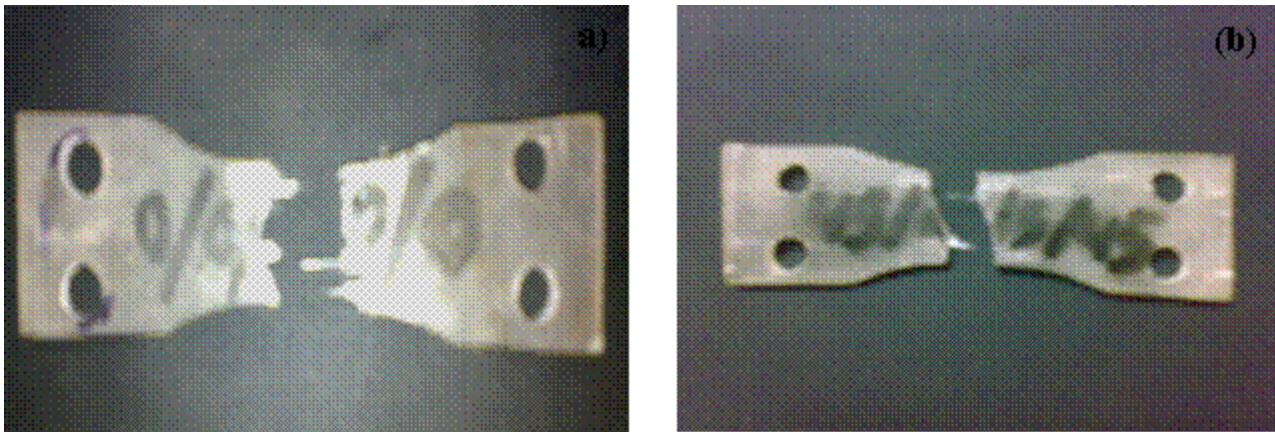


Fig.3. (a) Photograph of failed GFRP specimens of $[0^\circ]_3$ lamina orientation. (b) Photograph of failed GFRP specimens of $[45^\circ]_3$ lamina orientation.

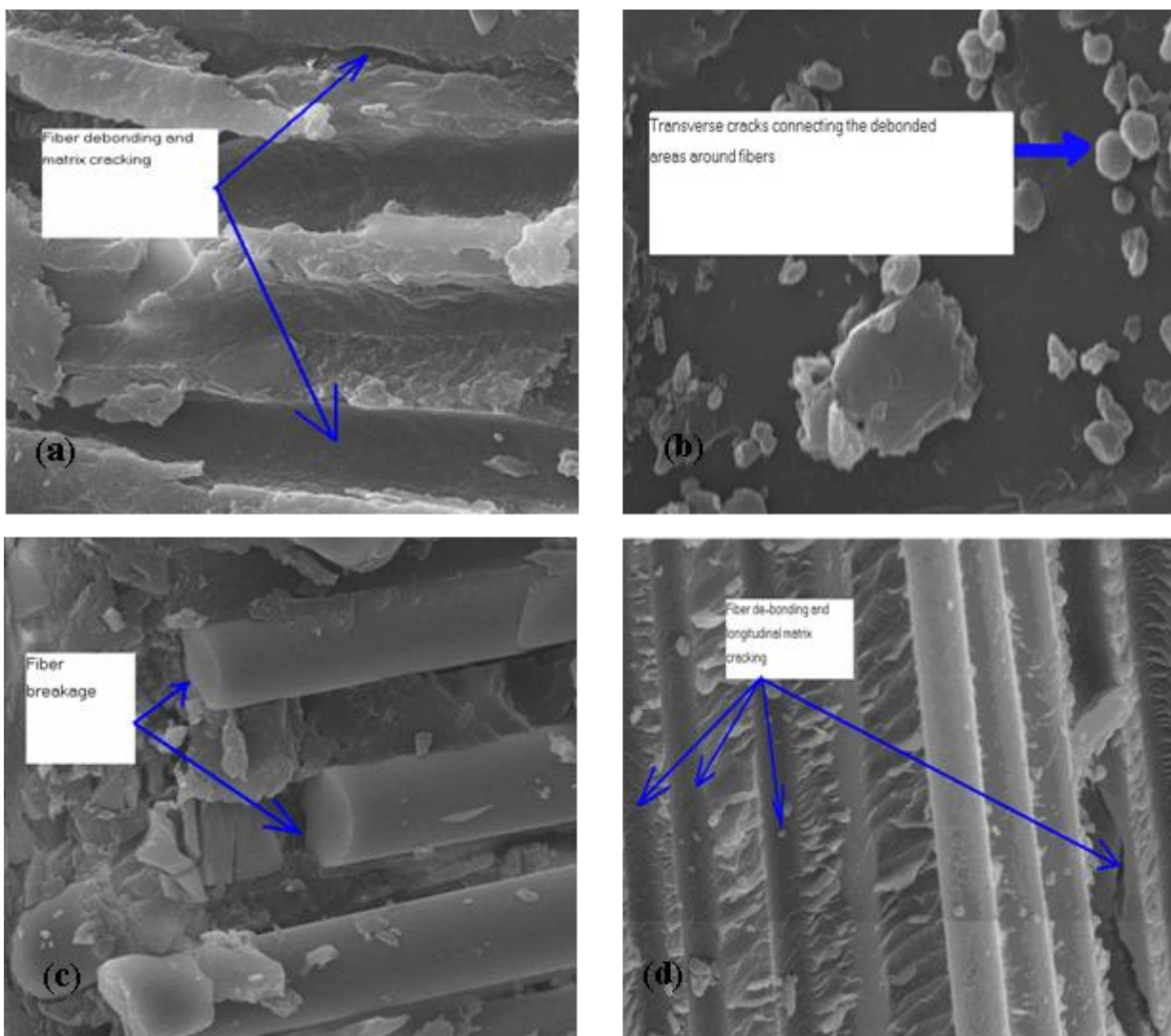


Fig.4. (a) SEM image of failed GFRP specimen of $[0^\circ]_3$ tested at 32MPa (b) Cross-sectional SEM images of failed GFRP specimen of $[0^\circ]_3$ tested at 32 MPa (c) SEM image of failed GFRP specimen of $[0^\circ]_3$ tested at 32 MPa showing fiber breakage (d) SEM image of failed GFRP specimen of $[0^\circ]_3$ tested at 32 MPa showing fiber de-bonding and longitudinal matrix cracking

(d) SEM image of failed GFRP specimen of $[45^\circ]_3$ tested at 19 MPa showing fiber pullout

4. Analysis and discussion of fatigue test results

The complete fatigue-life data obtained at various stress levels for GFRP specimens with different lamina orientation are listed in ascending order in Tables 4, 5 and 6 respectively

Table 4. Fatigue data for (GFRP) of $[0^\circ]_3$

Stress level ' σ '			
32 MPa	32 MPa	32 MPa	32 MPa
Cycles to failure(N)			
1444109	1444109	1444109	1444109
1615846	1615846	1615846	1615846
1694728	1694728	1694728	1694728
1736601	1736601	1736601	1736601
1788957	1788957	1788957	1788957
1833581	1833581	1833581	1833581
1859516	1859516	1859516	1859516
1916020	1916020	1916020	1916020
1945808	1945808	1945808	1945808
1963812	1963812	1963812	1963812

Table 5. Fatigue data for (GFRP) of $[45^\circ]_3$

Stress level ' σ '			
21 MPa	21 MPa	21 MPa	21 MPa
Cycles to failure(N)			
395458	395458	395458	395458
519996	519996	519996	519996
584655	584655	584655	584655
620726	620726	620726	620726
668344	668344	668344	668344
710068	710068	710068	710068
735360	735360	735360	735360
792136	792136	792136	792136
822811	822811	822811	822811
842170	842170	842170	842170

Table 6. fatigue data for (GFRP) of $[90^\circ]_3$

Stress level ' σ '			
16 MPa	16 MPa	16 MPa	16 MPa
Cycles to failure(N)			
323966	323966	323966	323966
755962	755962	755962	755962
1079941	1079941	1079941	1079941
1295985	1295985	1295985	1295985
1619944	1619944	1619944	1619944
1944017	1944017	1944017	1944017
2159733	2159733	2159733	2159733

2699604	2699604	2699604	2699604
3023431	3023431	3023431	3023431
3239664	3239664	3239664	3239664

4.1. Statistical analysis of fatigue-life data

The statistical analysis of fatigue-life results was carried out using a two-parameter Weibull distribution function which is characterized by a probability density function (PDF), $f(n)$; and the cumulative distribution function (CDF), $F(n)$ as follows

$$f(n) = \frac{\alpha}{\beta} \left(\frac{n}{\beta}\right)^{\alpha-1} \exp\left[-\left(\frac{n}{\beta}\right)^\alpha\right] \tag{1}$$

$$F(n) = 1 - \exp\left[-\left(\frac{n}{\beta}\right)^\alpha\right] \tag{2}$$

where, n = specific value of the random variable N ; α = shape parameter or Weibull slope at stress level σ and β = scale parameter or characteristic life at the same stress level. There are different methods for determination of the parameters α and β such as: graphical, moments, and maximum likelihood. In the following, the graphical and moments methods are employed to show that the statistical distribution of fatigue-life data at a certain stress level σ follows the two-parameter Weibull distribution. The parameters of the Weibull distribution are then obtained by the two methods.

4.2. Analysis of fatigue-life data by graphical method

The probability of survival or survivorship function or reliability function, $L_R(n)$, may be defined as $L_R(n) = 1 - F(n)$. Upon substituting of the value of $F(n)$ in Eq. (2) gives:

$$L_R(n) = \exp\left[-\left(\frac{n}{\beta}\right)^\alpha\right] \tag{3}$$

taking the logarithm twice of both sides of Eq. (3), it can be rewritten as

$$\ln\left[\ln\left(\frac{1}{L_R}\right)\right] = \alpha \ln(n) - \alpha \ln(\beta) \tag{4}$$

Equation (4) represents a linear relationship between $\ln[\ln(1/L_R)]$ and $\ln(n)$. In order to obtain a graph of Eq. (4), the fatigue-life data corresponding to a particular stress level are first arranged in ascending order of cycles to failure and the empirical survivorship function L_R for each fatigue-life data is obtained from the following relation [12]:

$$L_R = 1 - \left[\frac{(i-0.3)}{(k+0.4)}\right] \tag{5}$$

Where i denotes the failure order number and k represents the number of data points in a data sample under consideration. The empirical survivorship function in the form of $\ln[\ln(1/L_R)]$ for each fatigue-life data is then plotted on a graph with the corresponding fatigue lives $\ln(N)$, which represent a linear trend. It can then be assumed that fatigue-life data for that particular stress level follows the two-parameter Weibull distribution. The slope of the line provides an estimate of shape parameter α . One such typical graph for fatigue-life data at stress level $\sigma = 7$ MPa for GFRP specimen of $[90^\circ]_3$ lamina orientation is shown in Fig.5. The approximate straight line plot in Fig. 5 with statistical correlation coefficient of 0.98 indicates that the two-parameter Weibull distribution is a reasonable assumption for the statistical distribution of fatigue-life at this stress level.

Similar trends are observed for GFRP specimens of $[0^\circ]_3$ and $[45^\circ]_3$ lamina orientation at different stress levels with correlation coefficient exceeding 0.95. The parameters obtained by this method are summarized in tables 7, 8 and 9.

4.3. Parameter estimation by method of moments

Estimating parameters by method of moments requires finding the appropriate sample moments, such as sample mean and sample variance. The moments of Weibull distribution may be written in following forms

$$E(n) = \beta \Gamma\left(\frac{1}{\alpha} + 1\right) \tag{6}$$

and $E(n^2) = (\beta)^2 \Gamma\left(\frac{2}{\alpha} + 1\right)$ (7)

where $\Gamma(\cdot)$ is the gamma function and E denotes expectation. Noting that the mean of the data sample under consideration at a given stress level σ , $\mu = E(n)$ and the variance of the data sample under consideration at the same stress level σ , $\sigma_s^2 = E(n^2) - \mu^2$, Combining Eq.(6) and Eq.(7) gives:

$$\left(\frac{\sigma_s}{\mu}\right)^2 = \frac{\Gamma(\frac{2}{\alpha} + 1)}{\Gamma(\frac{1}{\alpha} + 1)^2} - 1 \tag{8}$$

Where $\sigma_s/\mu = CV$ represents the coefficient of variation of the fatigue data sample under consideration at a given stress level σ and σ_s is the standard deviation of the data sample under consideration. Since it is difficult to obtain the value of shape parameter α from Eq. (8), it can be reduced to a simple expression as follows [13]:

$$\alpha = (CV)^{-1.08} \tag{9}$$

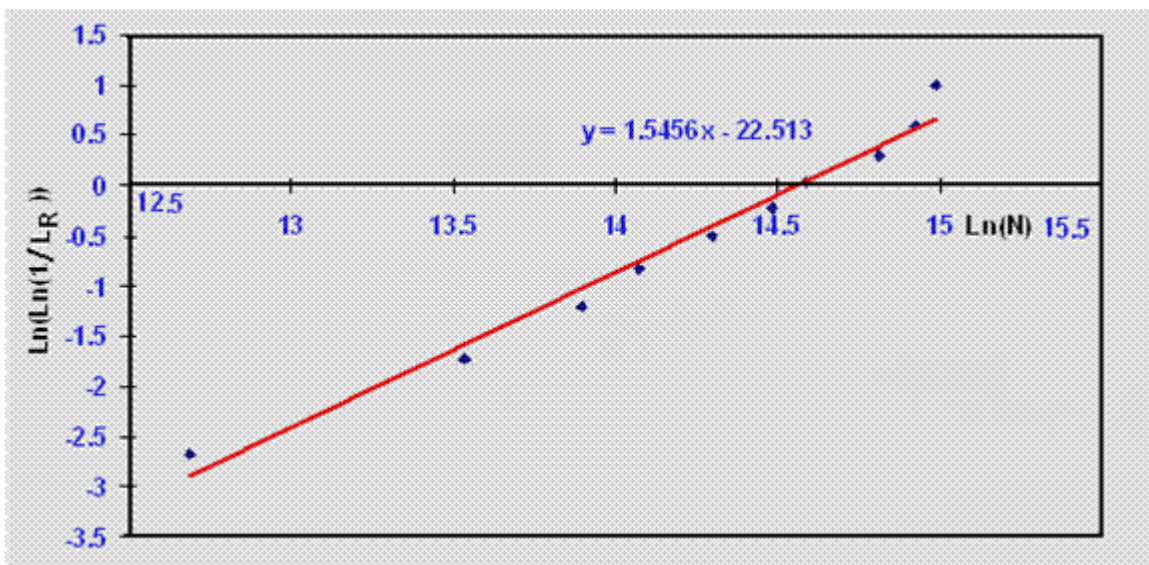


Fig.5. Graphical analysis of fatigue life data for GFRP specimen of $[90^\circ]_3$ lamina orientation at stress level 7 MPa

The parameter β can be estimated from Eq. (9) by substituting μ for E (n) in Eq. (6):

$$\beta = \frac{\mu}{\Gamma\left(\frac{1}{\alpha} + 1\right)} \tag{10}$$

The parameters obtained by this method for GFRP with the three different lamina orientations at different stress levels are also listed in tables 7, 8 and 9, respectively. It is seen that higher shape parameters are observed at higher stress levels, with less scatter in the fatigue-life data indicating a more uniform damage mechanism. Similar results have been reported earlier by other investigators for different materials [14p].

Table 7. Values of Weibull parameters for fatigue-life data of GFRP of [0°]3

Stress level	σ=32 MPa		σ=31 MPa		σ=30.5 MPa		σ=30 MPa	
	α	β	α	β	α	β	α	β
Graphical method	20.069	3189.65	14.747	69051.32	12.977	347839.9	11.575	1853951
Method of moments	23.55867	3184.5	17.04915	68892	14.92447	347200	13.25523	1850700
Average	21.81384	3187.075	15.89808	68971.66	13.95074	347520	12.41512	1852326

Table 8. Values of Weibull parameters for fatigue-life data of GFRP of [45°]3

Stress level	σ=21 MPa		σ=20 MPa		σ=19.5 MPa		σ=19 MPa	
	α	β	α	β	α	β	α	β
Graphical method	7.5156	2481.97	5.816	35837.88	5.207	154708.66	4.7056	730874.9
Method of moments	8.502116	2474.2	6.573249	35672	5.89204	153850	5.336373	726090
Average	8.008858	2478.085	6.194625	35754.94	5.54952	154279.3	5.020987	728482.5

Table 9. Values of Weibull parameters for fatigue-life data of GFRP of [90°]3

Stress level	σ=16 MPa		σ=14 MPa		σ=10 MPa		σ=7 MPa	
	α	β	α	β	α	β	α	β
Graphical method	1.5459	2724.269	1.5458	12280.41	1.5457	196220.5	1.5456	2117749
Method of moments	1.949765	2631.6	1.949642	11857	1.949881	189460	1.950005	2046000
Average	1.747833	1316.573	1.747771	5929.273	1.747891	94730.77	1.747953	1023001

4.4. Failure probability and S–N relationships

The S–N relationships reported by earlier investigators do not incorporate failure probability P_f , which is an important parameter in fatigue-life studies. The Weibull distribution has been employed herein to incorporate the failure probability into S–N relationships for GFRP’s. Substituting $1 - P_f = L_R$ in Eq. (4), the following relation is obtained

$$\ln \left[\ln \left(\frac{1}{1 - P_f} \right) \right] = \alpha \ln(n) - \alpha \ln(\beta) \tag{11}$$

Rearranging,

$$n = \ln^{-1} \left[\frac{\ln \left\{ \ln \left(\frac{1}{1 - P_f} \right) \right\} + \alpha \ln(\beta)}{\alpha} \right] \tag{12}$$

Thus, using the average values of the parameters of Weibull distribution for fatigue-life at any stress level (as listed in Tables 7, 8 and 9), Eq. (12) has been used to calculate the fatigue lives at a given stress level corresponding to different failure probabilities. The calculated values of fatigue lives for GFRP with the three different lamina orientations for failure probabilities of $P_f = 0.2, 0.3, 0.5, 0.8$ and 0.95 , are plotted in Figs. 6, 7 and 8 respectively for GFRP to obtain $P_f - S - N$ diagrams

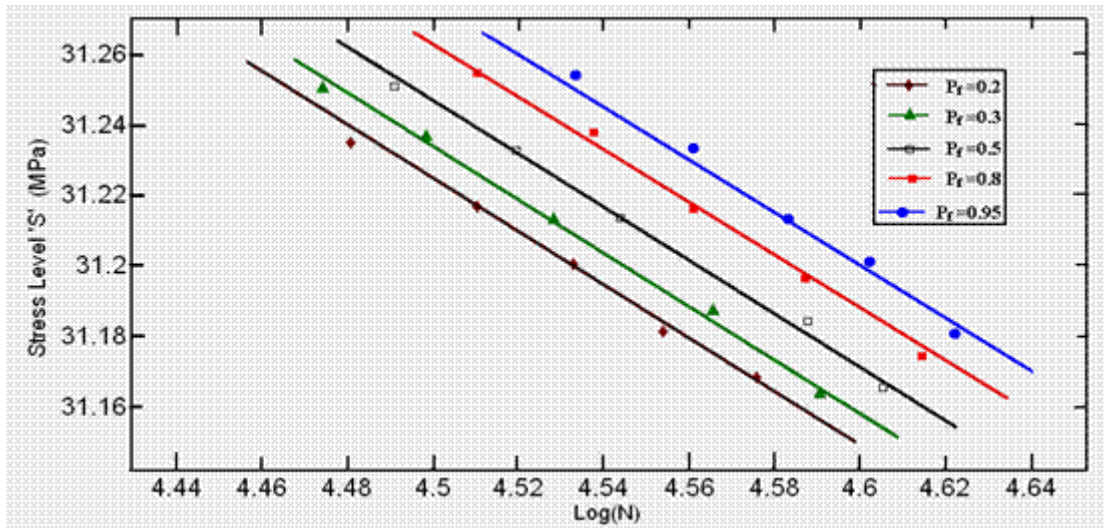


Fig.6. $P_f - S - N$ diagram for GFRP specimen of $[0^\circ]_3$ lamina orientation

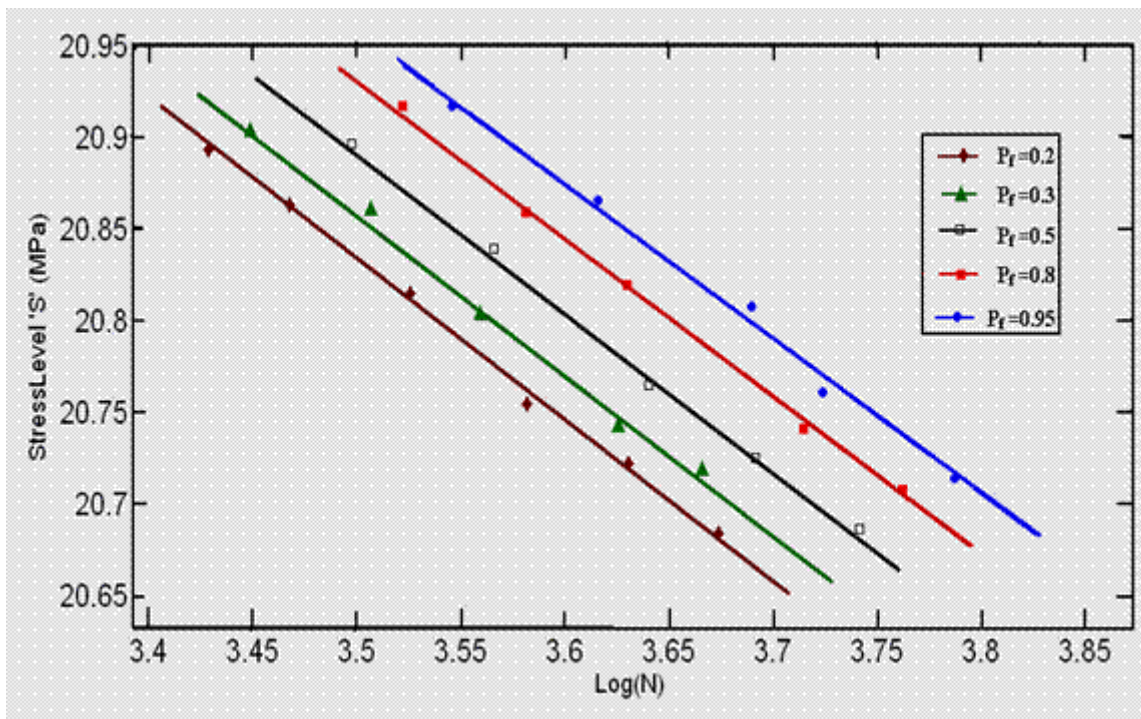


Fig.7. $P_f - S - N$ diagram for GFRP specimen of $[45^\circ]_3$ lamina orientation

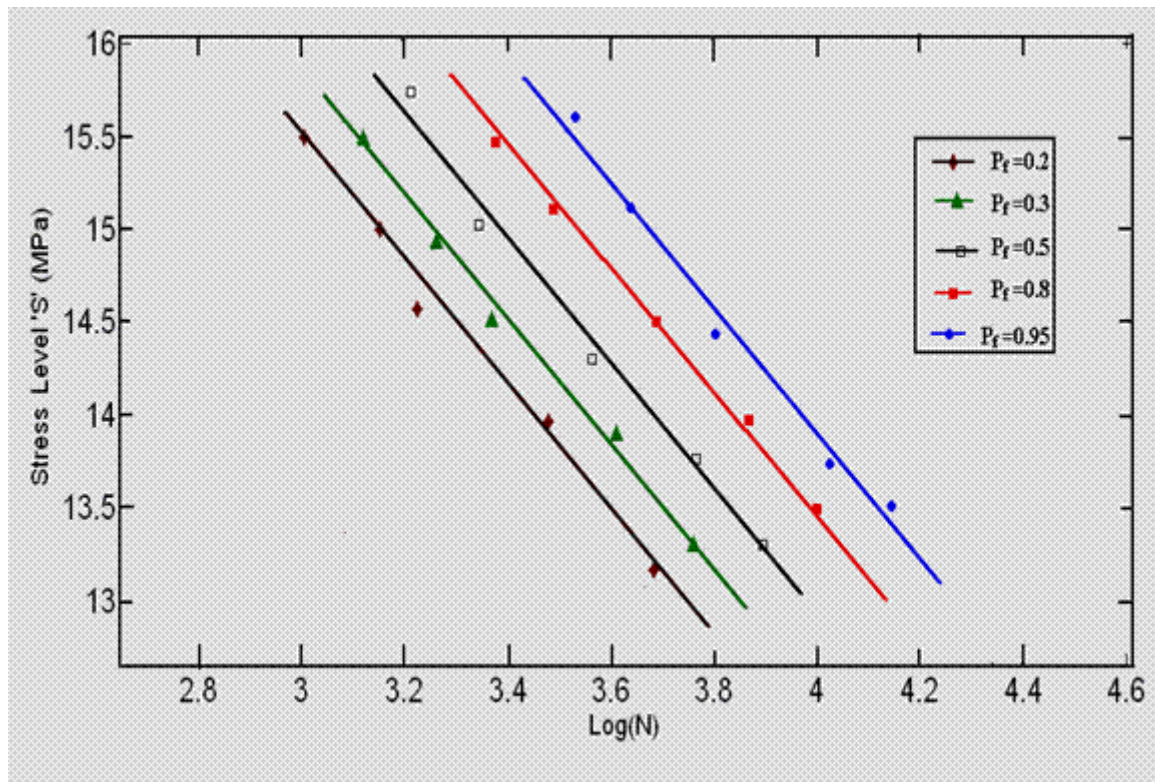


Fig.8. P_f -S-N diagram for GFRP specimen of $[90^\circ]_3$ lamina orientation

5. Conclusions

In the present work, the statistical analysis of plane bending fatigue life data in composite structure is established with the lowest residual errors. The following conclusions may be summarized:

1. For all investigated laminates, different modes of failure mechanisms are observed at low and high fatigue stress levels, which establish different damage mechanisms.
2. The probabilistic distribution of fatigue-life for GFRP with different lamina orientations at any stress level can be approximately modeled using two-parameter Weibull distribution with statistical correlation coefficient values exceeding 0.95.
3. The shapes of the Weibull distribution for fatigue-life of GFRP are different for different levels of the applied fatigue stress. The two methods used to estimate the parameters of Weibull distribution yield almost similar results.
4. Higher shape parameters are observed at higher stress levels with less scatter in the fatigue-life data indicating a more uniform damage mechanism.
5. Using two-parameter Weibull distribution, the P_f -S-N relationships have been generated for GFRP. These relationships can be used by designers to obtain the fatigue strength of GFRP at the desired level of failure probability.

References:

- [1] Shokrieh M and Lessard L. "Mutiaxial fatigue behavior of unidirectional plies based on uniaxial fatigue experiments-I. Modeling" Int J Fatigue 1997; 19(3):201-7.
- [2] Chen AS, Matthews FL. Composites 1993; 34:395-406.
- [3] Fround MS. Multiaxial fatigue. In: Miller KJ, Brown MW, editors. ASTM STP 853. Philadelphia: American Society for Testing and Materials; 1985. p. 381-95.

- [4] Diao X, Lessard L and Shokrieh M. "Statistical model for multiaxial fatigue behavior of unidirectional plies" *Compos Sci Technol* 1999; 59:2025–35.
- [5] Joris D and Paepegam WV. "Fatigue damage modeling of fiber reinforced composite materials – review. *Appl Mech Rev* 2001; 54(4):279–300.
- [6] Tsai SW. *Composite design*, 4th ed. Think Composites; 1988.
- [7] Lee J, Harris B, Almond DP and Hammett F. "Fiber composite fatigue life determination" *Composites A* 1997; 28:5–15.
- [8] ASTM Special Publication 91-A, A guide for fatigue testing and the statistical analysis of fatigue data. ASTM 1963; 83.
- [9] Raif Sakin İrfan Ay "Statistical analysis of bending fatigue life data using Weibull distribution in glass-fiber reinforced polyester composites" *Materials and Design* 29 (2008) 1170–1181
- [10] Raman Bedi and Rakesh Chandra "Fatigue-life distributions and failure probability for glass-fiber reinforced polymeric composites" *Composites Science and Technology* 69 (2009) 1381–1387
- [11] Ahmed Abd El-Hamid Hamada "vibration and damping analysis of beams with composite coats" *composite structures* 32(1995) 33-38
- [12] Kennedy JB, Neville AM." *Basic statistical methods for engineers and scientists*" A Dun-Donnelley Publishers; 1986. 613.
- [13] Wirsching PH, Yao JTP. *Statistical methods in structural fatigue*. J Struct Div Proc ASCE 1970:1201–19.
- [14] Lee J, Harris B, Almond DP and Hammett F. "Fiber composite fatigue life determination" *Composites A* 1997; 28:5–15.

Nomenclature:

CV	coefficient of variation of the data sample under consideration
E	expectation
f (n)	probability distribution function
F (n)	cumulative distribution function
i	order number of the data point in a sample under consideration
k	total number of data points in a sample under consideration or sample size
L_R	survivorship function/survival probability/reliability function
n	number of cycles
N	number of cycles to failure or fatigue-life.
P_f	failure probability
β	characteristic life or scale parameter of Weibull distribution
α	shape parameter of the Weibull distribution or Weibull slope
σ	applied fatigue stress level
σ_s	standard deviation of the data sample under consideration
σ_{ult}	ultimate tensile strength
$\Gamma ()$	gamma function
μ	mean value of the data sample under consideration